# CD38-expressing myeloid-derived suppressor cells promote tumor growth in a murine model of esophageal cancer

Karakasheva, Tatiana A.; Waldron, Todd J.; Eruslanov, Evgeniy; Kim, Sang-Bae; Lee, Ju-Seog; O'Brien, Shaun; Hicks, Philip D.; Basu, Devraj; Singhal, Sunil; Malavasi, Fabio; Rustgi, Anil K.. CD38-expressing myeloid-derived suppressor cells promote tumor growth in a murine model of esophageal cancer. CANCER RESEARCH. 75 (19) pp: 4074-4085.
DOI: 10.1158/0008-5472.CAN-14-3639

# CD38-Expressing Myeloid-Derived Suppressor Cells Promote Tumor Growth in a Murine Model of Esophageal Cancer

Todd J. Waldron[1,2,*], Tatiana A. Karakasheva[1,2,*], Evgeniy Eruslanov[3], Ju-Seog Lee[4], Shaun O'Brien[3], Devraj Basu[5,6], Sunil Singhal[3,6], Fabio Malavasi[7**], and Anil K. Rustgi[1,2,8**]

[1]Division of Gastroenterology; Department of Medicine; University of Pennsylvania; Philadelphia, PA USA
[2]Abramson Cancer Center; University of Pennsylvania; Philadelphia, PA USA
[3]Thoracic Surgery Research Laboratory, Department of Surgery; Hospital of the University of Pennsylvania School of Medicine; Philadelphia, PA USA;
[4]Department of Systems Biology, MD Anderson Cancer Center, Houston, Texas
[5]Department of Otorhinolaryngology - Head and Neck Surgery, University of Pennsylvania, Philadelphia, PA, USA
[6]Surgery Service; Philadelphia Veterans Affairs Medical Center; Philadelphia, PA USA
[7]Lab of Immunogenetics, Department of Medical Sciences, University of Torino Medical School; Torino, Italy
[8]Department of Genetics; University of Pennsylvania; Philadelphia, Pennsylvania

[*]These authors contributed equally to this work.
**Co-corresponding senior authors.

Running title: CD38 function in MDSCs

Keywords: CD38, myeloid derived suppressor cells, immature myeloid cells, iNOS, NFκB

Address reprints to:
Anil K. Rustgi, University of Pennsylvania, 951 BRB II/III, 421 Curie Boulevard, Philadelphia, PA 19104. Phone: 215-898-0154; Fax: 215-573-5142; E-mail: anil2@mail.med.upenn.edu.

**Funding:**

This work was supported by the National Institutes of Health/NCI grant P01-CA098101 (AKR, TW, TK), National Institutes of Health/NCI grant U01-CA14305603 (AKR), National Institutes of Health/NIDDK (T32-DK007066) (TW), National Institutes of Health (F32-CA162719) (TW), National Institutes of Health/NIDDK Center for Molecular Studies in Digestive and Liver Diseases (P30-DK050306), American Cancer Society (RP-10-033-01-CCE), National Institutes of Health NIH/NIDCR (K08-DE022842) (DB), National Institutes of Health (Transformative R01-CA163256-01) (SS), Italian Ministry of Education, University and Research (Progetto PRIN and FIRB) (FM) and by the Fondazione Ricerca in Medicina Sperimentale (FIRMS) (FM).

The authors have no conflicts of interest to disclose.

## Abstract

Myeloid derived suppressor cells (MDSCs) are an immunosuppressive population of immature myeloid cells found in advanced stage cancer patients and mouse tumor models.  Production of inducible nitric oxide synthase (iNOS) and arginase, as well as other suppressive mechanisms, allow MDSCs to suppress T cell-mediated tumor clearance and foster tumor progression. Using an unbiased global gene expression approach in conditional p120-catenin knockout mice (*L2-cre;p120ctn*$^{f/f}$), a model of oral-esophageal cancer, we have identified CD38 as playing a vital role in MDSC biology, previously unknown.  CD38 belongs to the ADP-ribosyl cyclase family and possesses both ectoenzyme and receptor functions.  It has been described to function in lymphoid and early myeloid cell differentiation, cell activation and neutrophil chemotaxis.  We find that CD38 expression in MDSCs is evident in other mouse tumor models of esophageal carcinogenesis, and CD38$^{high}$ MDSCs are more immature than MDSCs lacking CD38 expression, suggesting a potential role for CD38 in the maturation halt found in MDSC populations.  CD38$^{high}$ MDSCs also possess a greater capacity to suppress activated T cells, and promote tumor growth to a greater degree than CD38$^{low}$ MDSCs, likely as a result of increased iNOS production. Additionally, we have identified novel tumor-derived factors, specifically IL-6, IGFBP-3 and CXCL16, which induce CD38 expression by MDSCs *ex vivo*. Finally, we have detected an expansion of CD38-positive MDSCs in peripheral blood of advanced stage cancer patients and validated targeting CD38 *in vivo* as a novel approach to cancer therapy.

## Introduction

The immune system (both innate and adaptive) plays an essential role in limiting tumor growth, and therefore, tumor progression requires escape from immune surveillance. One mechanism that allows for tumor escape is the activation and expansion of immunosuppressive cell populations, including but not limited to, regulatory T cells (Tregs) and myeloid derived suppressor cells (MDSCs) (1), the latter also referred to as immature myeloid cells (IMCs). Certain therapeutics have demonstrated potential efficacy against MDSCs (2); however, the need for more selective anti-MDSC therapeutics remains.

MDSCs have been observed in a number of mouse tumor models and represent a heterogeneous population of immature monocytes and granulocytes that are identified by their $CD11b^{+}Gr1^{+}$ phenotype in mice (3). In human disease, the first immature myeloid cell population with immunosuppressive capacity was described in head and neck cancer (4), and since then MDSCs have been documented in cancers of the esophagus, stomach, pancreas, lung, kidney, colon, skin, prostate, and breast (5–10). The immunophenotype of human MDSCs varies (11), however, their immunosuppressive mechanisms match those found in murine $CD11b^{+}Gr1^{+}$ MDSC populations.

MDSCs induce immune suppression primarily through inhibition of T cell-mediated tumor clearance (3), but can also promote inhibition of NK cells (12) and activation of Tregs (13). Arginase-1 (ARG1) and inducible nitric oxide synthase-2 (iNOS) provide the bulk of the enzymatic activity required for MDSCs to suppress T cell proliferation and activation of (3). ARG1 deprives T cells of arginine by converting L-arginine into urea and L-ornithine, thereby reducing expression of CD3ζ chain, which renders T cells unable to respond to activation signals (14). iNOS inhibits T cell function by a variety of mechanisms, including inhibition of JAK3/STAT5 signaling (15), MHC Class II expression (16) and induction of apoptosis (17).

CD38 expression is a common characteristic to several immunosuppressive cell types. Foxp3$^+$CD25$^+$CD4$^+$ Tregs expressing high CD38 levels possess a greater immunosuppressive activity than CD38$^{low}$ Tregs (18). CD38$^+$CD8$^+$ T cells suppress proliferation of CD4$^+$ effector T cells, which requires IFNγ secretion and cell-to-cell contact (19). Similarly, CD19$^+$CD24$^{hi}$CD38$^{hi}$ B cells inhibit differentiation of T helper 1 cells in an IL-10 dependent manner, and their dysfunction may play a role in autoimmune disorders such as systemic lupus erythematosus (20).

CD38 is a member of the ribosyl cyclase family and is expressed on the surface of diverse immune cells, including B cells, T cells, NK cells and myeloid cells (21). CD38 possesses independent ectoenzyme and receptor functions. As an ectozyme, CD38 catalyzes synthesis and hydrolysis of cyclic ADP-ribose (cADPR), converting NAD$^+$ to ADP-ribose (ADPR), as well as cADPR into ADPR (21,22). Furthermore, at acidic pH, CD38 catalyzes synthesis and hydrolysis of nicotinic acid adenine dinucleotide phosphate (NAADP) (21,22). Both reactions are essential for calcium signaling, specifically for mobilization of intracellular Ca$^{2+}$ (22). Receptor activity of CD38 has been documented in multiple immune cell types, where it is dependent on localization to the lipid rafts and association with professional signaling complexes (21). In both mouse and human myeloid cells, ligation of CD38 receptor leads to suppressed growth and survival resulting in loss of the most differentiated immune populations (23).

In this study we have identified CD38 as a novel marker for MDSCs that possess greater immunosuppressive capacity, thereby promoting tumor growth *in vivo.* We have identified a mechanistic role for CD38 in promoting expansion of the monocytic MDSC population, as well as in regulating expression of the effector molecule iNOS by these cells. Additionally, we have established for the first time that several cytokines, specifically IFNγ, TNFα, IGFBP-3, CXCL16 and IL-6, are capable of inducing CD38 expression in MDSCs. Finally, we have demonstrated that administration of an anti-CD38 monoclonal antibody slows disease progression in tumor-bearing mice. As we have detected an expansion of CD38-positive MDSC-like population in peripheral blood of advanced-stage cancer patients, this study introduces the concept of anti-CD38 monoclonal antibody therapy for potential treatment of certain solid tumors.

## Materials and Methods

### *Generation of MDSCs*

All animal studies were approved by the Institutional Animal Care and Use Committee (IACUC) at the University of Pennsylvania. Mice were housed under a 12-hour light/dark cycle and fed ad libitum. We have described the *L2-Cre;p120ctn*$^{f/f}$ mouse model of oral-esophageal cancer previously (24). We also used syngeneic subcutaneous transplantation models utilizing the HNM007 and AKR ESCC cell lines in either C57BL/6J (Jackson Labs) or *Cd38*$^{-/-}$ mice (gift from Dr. Eduardo Chini). For generation of MDSCs, *L2-Cre;p120ctn*$^{f/f}$ mice were aged until signs of preneoplasia and neoplasia were evident; subcutaneous tumor-bearing mice were aged until tumors reached a volume of 0.8cm$^3$. Spleens and bone marrow were harvested upon euthanasia for MDSC isolation.

### *Flow cytometry and cell sorting*

Single cell suspensions were prepared from mouse bone marrow or spleen by mechanical disruption.  Red blood cells were lysed, and the remaining leukocytes were washed with PBS, and resuspended in PBS + 2% FBS. For analysis of patient blood samples, peripheral blood mononuclear cells (PBMC) were separated using gradient centrifugation. Samples were analyzed on a FACScalibur (BD) or LSRII (BD).  Cell sorting for multiple markers was performed on a FACSAriaII (BD).  Data were analyzed using FlowJo (Treestar).

Peripheral blood from previously untreated, advanced stage HNC patients was obtained with informed consent under University of Pennsylvania IRB protocol #417200 or Philadelphia VA Medical Center protocol #01090.

*Histology*

Subcutaneous tumors were fixed in buffered formalin solution, paraffin-embedded and stained with hematoxylin and eosin (H&E). $CD11b^+Gr1^+$, $CD11b^+Gr1^+CD38^{low}$, and $CD11b^+Gr1^+CD38^{high}$ cells were sorted by flow cytometry. Cytospin preparations were stained using the Hema 3 system (Fisher Scientific).

*T cell suppression*

$CD11b^+Gr1^+$, $CD11b^+Gr1^+CD38^{low}$, and $CD11b^+Gr1^+CD38^{high}$ cell populations were sorted by flow cytometry. Antigen-specific $CD8^+$ T cell suppression was tested as described previously (24).

*Ex vivo MDSC differentiation*

Generation of MDSCs from bone marrow has been described previously (25). Cytokine concentrations used: 0.1 ng/ml (GM-CSF and IL-4), 10 ng/ml (TNFα and IFNγ), and 100 ng/ml (IL-6, CXCL16 and IGFBP-3). HNM007 or AKR conditioned medium (CM) were used at 50% v/v. Anti-CD38 monoclonal antibody and IgG2a isotype control were used at 10ug/ml.

*Colony formation and cell recovery assays*

Isolation of MDSCs from tumor-bearing *L2-cre;p120*$^{-/-}$ mice by magnetic cell sorting was described previously (24). 200,000 cells were seeded in each 35 mm plate containing 1 ml of methylcellulose-based medium containing factors that promote growth of granulocyte-macrophage progenitors (M3534; Stem Cell Technologies). Anti-CD38 monoclonal antibody and IgG2a isotype control were used at 10ug/mL. Colonies were counted after 7 days. For recovery assays, $5x10^5$ MDSCs were seeded in complete RPMI 1640 medium supplemented with antibodies; cells were quantified by Trypan exclusion using a Countess automated cell counter (Invitrogen).

*Cytokine array*

Media from *ex vivo* differentiation cultures were collected and snap-frozen after 1 or 5 days of culture. Mouse cytokine array C3 kit was used according to the manufacturer's protocol. Results were quantified using the ImageJ protein array analyzer and normalized to positive controls to allow for comparison of relative expression levels.

*ESCC/MDSC co-transplantation and anti-CD38 therapeutic study*

C57BL/6J recipient mice from Jackson Labs were injected subcutaneously with a mixture of $2.5x10^5$ syngeneic HNM007 tumor cells with either $2.5x10^5$ CD38$^{low}$ or CD38$^{hi}$ MDSCs obtained from HNM007 tumor-bearing C57BL/6J mice. Recipient mice injected with $2.5x10^5$ syngeneic HNM007 tumor cells alone served as controls. For antibody treatment experiments, anti-CD38 monoclonal antibody or IgG2a isotype control antibody were administered intraperitoneally every 48 hours starting on day 5 post-injection.  Measurements were taken every 2-3 days once tumors became palpable.

*Statistical analysis*

The Student's t test was used to whether there is significant difference between two experimental groups ($p \leq 0.05$ was considered statistically significant).

Additional details can be found in Supplementary Materials and Methods.

## Results

### *Myeloid-derived suppressor cells from tumor-bearing L2-Cre;p120$^{f/f}$ mice exhibit elevated CD38 expression*

We have previously demonstrated that MDSCs play a fundamental role in tumor initiation and progression in a spontaneous genetic mouse model of ESCC (*L2-Cre;p120$^{f/f}$;* referred to hereafter as *p120$^{-/-}$*) (24). Here we sought to identify genes associated with an immature myeloid phenotype that contribute to the tumor promoting activities of MDSCs, thereby providing a platform to elucidate underlying molecular mechanisms. To that end, we performed microarray analysis of splenic MDSCs from 6-8 month old tumor-bearing *p120$^{-/-}$* mice and age-matched littermate controls (Supplementary Fig.1). Among the 964 genes showing differential expression between the two groups (Figure 1A), we identified *Cd38* (ranked fifth highest among all genes tested (Supplementary Table 1))as a candidate gene of interest, as it has roles in both innate and adaptive immunity in mice and humans, including, but not limited to chemotaxis of murine and human neutrophils (26,27), early myeloid differentiation (23) and lymphoid cell activation (28). We validated enhanced *Cd38* mRNA and protein expression in MDSCs from tumor-bearing mice as compared to those isolated from control mice (Fig. 1B-D). We also observed increased CD38 in splenic MDSCs isolated from *L2-IL1β* mice, a model of Barrett's esophagus and esophageal adenocarcinoma (29) (Supplementary Fig. 2).

*CD38 expression correlates with ESCC progression and expansion of monocytic MDSC population*

To determine the kinetics of CD38 expression in MDSCs, we analyzed splenic $CD11b^+Gr1^+$ populations from non-diseased (8 weeks) and tumor-bearing (6-8 months) *p120*$^{-/-}$ mice, as well as control mice. $CD11b^+Gr1^+$ cells were slightly more abundant in spleens of non-diseased *p120*$^{-/-}$ mice and markedly elevated in spleens of tumor-bearing *p120*$^{-/-}$ mice, compared to control mice (Fig 2A). CD38 expression was markedly increased only in splenic MDSCs from tumor-bearing *p120*$^{-/-}$ mice (Fig. 2B), while a more mature subset of myeloid cells ($CD11b^+Gr1^-$) exhibited no change in CD38 levels (Fig 2B).

We next tested two murine ESCC cell lines (AKR (30) and HNM007 (31)) for their ability to generate MDSCs *in vivo* using a syngeneic transplant model. We observed dramatically increased CD38 levels in all myeloid populations from spleens of HNM007 tumor-bearing mice, yet in AKR tumor-bearing mice CD38 levels were overall lower (Fig. 2C, Supplementary Fig. 3). Interestingly, while both cell lines induced expansion of myeloid populations in spleens of tumor-bearing mice, it was significantly more pronounced ($p<0.0009$) in HNM007 tumor-bearing mice (Fig. 2D). Furthermore, we observed differences in distribution of granulocytic and monocytic MDSCs (G-MDSC and M-MDSC, respectively), as well as mature monocytes (Fig. 2D). G-MDSCs ($CD11b^+Ly6G^+$) were less abundant ($p<0.02$) in HNM007 tumor-bearing mice, compared to AKR. There also was a trend of M-MDSC ($CD11b^+Ly6C^+$) expansion, accompanied by a significant increase in mature monocytes ($CD11b^+Ly6C^-Ly6G^-$) in HNM007, compared to AKR tumor-bearing and control mice ($p<0.02$). These findings suggest that CD38 may be relevant to M-MDSC expansion in tumor-bearing mice.

### *CD38$^{high}$ MDSCs possess greater immunosuppressive and tumor-promoting capacity than CD38$^{low}$ MDSCs*

Since the CD38$^{high}$ MDSC population expands in tumor-bearing mice, we hypothesized that CD38$^{high}$ MDSCs possess greater immunosuppressive potential than CD38$^{low}$ MDSCs. To test this, we sorted CD38$^{high}$ and CD38$^{low}$ MDSCs from HNM007 tumor-bearing mice and assessed their capacity to suppress OT-1 T cell growth following stimulation with cognate antigen. CD38$^{high}$ MDSCs demonstrated significantly greater T cell suppressive capacity, compared to their CD38$^{low}$ counterparts (Fig. 3A), at 2:1 OT-1 to MDSC ratio, while a trend of increased suppression was observed at 1:1 and 4:1 ratios.

Next we evaluated the impact of co-injection of CD38$^{high}$ MDSCs with HNM007 cells on tumor growth. Tumor volumes in CD38$^{high}$ group were significantly larger than CD38$^{low}$ tumors on days 6 and 10 (Fig. 3B), and larger than control HNM007 tumors on days 8, 10 and 13 (Fig. 3B). No difference in size was detected between the CD38$^{low}$ and control HNM007 tumors. Furthermore, CD38$^{high}$-injected tumors were characterized by increased necrosis and inflammatory infiltrate, compared to controls (Fig. 3C, D). These results suggest that CD38$^{high}$ MDSCs may possess greater tumor-promoting capacity than CD38$^{low}$ MDSCs *in vivo*.

Next we investigated whether CD38 is required for the immunosuppressive function of MDSCs by analyzing the capacity of MDSCs from *Cd38*$^{-/-}$ and *Cd38*$^{+/+}$ (*wt*) mice bearing HNM007 tumors to suppress OT-1 T cell proliferation. Interestingly, *Cd38*$^{-/-}$ MDSCs exhibited significantly reduced immunosuppressive capacity at 1:1 and 4:1 OT-1 to MDSC ratios (Fig. 3E).

### *CD38$^{high}$ MDSCs are phenotypically different from the CD38$^{low}$ subset*

Next we analyzed CD38$^{high}$ and CD38$^{low}$ splenic MDSCs from tumor-bearing *p120*$^{-/-}$ mice via microarray (Supplementary Fig.4) and detected differential expression of 498 genes (Fig. 4A, Supplementary Table 2). Among genes with the greatest increase in expression, was inducible nitric oxide synthase (*iNos*). qPCR analysis further revealed that *iNos expression* was significantly elevated in CD38$^{high}$ MDSCs compared to CD38$^{low}$ MDSCs, while expression of arginase 1 (*Arg1*) and NADPH oxidase subunit (*Nox2*) , two additional mediators of MDSC suppressive function, was comparable in the subpopulations (Fig. 4B). iNOS protein expression was also validated in CD38$^{high}$ MDSCs (Fig 4C). Since *iNos* is a target of NFκB transactivation (32), we evaluated phospho-NFκB levels in CD38$^{high}$ and CD38$^{low}$ MDSCs and found elevated phospho-NFκB (p65) levels in the CD38$^{high}$ population (Fig. 4C). To test whether iNOS contributes to the increased immunosuppressive capacity of CD38$^{high}$ MDSCs, we used an iNOS inhibitor (L-NMMA), and found that it completely abrogated OT-1 T cell suppression mediated by CD38$^{high}$ MDSCs (Fig. 4D). Finally, the CD38 inhibitor AraF-NAD (33) partially rescued OT-1 T cell proliferation (Fig. 4E), suggesting that CD38 enzymatic activity is required for immunosuppressive capacity of CD38$^{high}$ MDSCs. Furthermore, iNOS expression was decreased in MDSCs isolated from the spleens of HNM007 tumor-bearing *Cd38*$^{-/-}$ (Fig. 4F).

Morphological assessment of sorted CD38$^{low}$ and CD38$^{high}$ MDSCs revealed that the CD38$^{high}$ population consists of more immature cells, such as promyelocytes (~10%), myelocytes (5-10%) and metamyeloctyes (5-10%), and band cells (~70%), whereas the CD38$^{low}$ population consists of band cells (<10%) and mature neutrophils (>90%) (Fig. 4G), demonstrating that CD38$^{high}$ MDSCs are morphologically more immature than CD38$^{low}$ MDSCs.

*IFN $\gamma$, TNF $\alpha$, CXCL16, IGFBP-3 and IL-6 induce CD38 expression*

Since we found that MDSCs from HNM007 tumor-bearing mice have increased CD38 expression, compared to AKR tumors (Fig. 2C), we sought to understand signaling pathways underlying this phenotype. We performed *ex vivo* bone marrow differentiation assays using GM-CSF, IL-4 (both required for CD11b$^+$Gr1$^+$ generation from bone marrow progenitors (25)) and conditioned media (CM) from either HNM007 or AKR cells. Only HNM007 CM induced CD38 expression (Fig. 5A). Since IFNγ and TNFα are key components of the pro-inflammatory milieu and are known activators of CD38 transcription (34), we used these cytokines in *ex vivo* differentiation assays. Interestingly, both factors, individually or in combination, induced CD38 expression in CD11b$^+$Gr1$^+$ cells (Fig. 5A). A cytokine array using CM from *ex vivo* differentiation experiments revealed several factors, including CXCL16 and IGFBP-3 that were present at higher levels in HNM007 cultures as compared to AKR cultures (Fig.5B). In addition, the pro-inflammatory cytokine IL-6, a predicted activator of CD38 transcription (34), was elevated in HNM007 cultures, albeit not as dramatically as CXCL16 or IGFBP-3 (Fig. 5B). Next we investigated the capacity of recombinant IL-6, CXCL16 and IGFBP-3 to increase CD38 expression *ex vivo*. Interestingly, addition of IL-6, CXCL16 and IGFBP-3 in combination induced CD38 expression in AKR CM cultures (Fig. 5C).

### *Cross-linking of CD38 by an agonistic antibody impairs expansion and survival of $CD11b^+Gr1^+$ cells in vitro and suppresses tumor growth in vivo*

To test whether cross-linking of CD38 with a monoclonal antibody has an effect on MDSC function(s), MDSCs from spleens of tumor-bearing *p120*$^{-/-}$ mice were cultured in methylcellulose-based medium in the presence of an anti-CD38 monoclonal antibody (NIM-R5) or isotype control (IgG2a). Addition of anti-CD38 antibody inhibited growth of colonies from splenic MDSCs, and the effect of anti-CD38 antibody remained unchanged regardless of whether splenocytes were pre-sorted (Fig. 6A and 6B), demonstrating that the anti-CD38 antibody inhibits MDSC proliferation and survival *in vitro*. In suspension culture, sorted MDSCs survive only a few days, but their survival was further reduced in the presence of anti-CD38 antibody (Fig. 6C). We also tested whether CD38 cross-linking inhibits accumulation of $CD11b^+Gr1^+CD38^{high}$ cells *ex vivo* in the presence of HNM007 CM. Using an additional anti-CD38 antibody (clone 90), we observed a dose-dependent decrease in CD38 expression within the CD11b$^+$Gr1$^+$ population (Fig. 6D). Given that the proportion of CD11b$^+$Gr1$^+$ cells within the culture remained consistent (25-30%; data not shown), these data demonstrate that the CD11b$^+$Gr1$^+$CD38$^{high}$ population is likely depleted as a result of CD38 cross-linking. Lastly, anti-CD38 antibody treatment resulted in decreased tumor growth rate *in vivo* in a subcutaneous HNM007 transplant ESCC model as compared to isotype control (Fig. 6E). In aggregate, these data demonstrate the importance of CD38 for MDSC-mediated ESCC progression and suggest targeting CD38 as an approach to ESCC therapy.

### *CD38 is expressed on human MDSC-like cell population that is expanded in peripheral blood of advanced-stage cancer patients*

To determine whether our findings may be relevant to human cancers, we analyzed CD38 expression in the CD15$^{hi}$CD33$^{lo}$ population of PBMCs from advanced stage head and neck cancer and non-small cell lung cancer patients and healthy donors. In contrast to our observations in mice, we found that CD38 expression levels were unchanged in CD15$^{hi}$CD33$^{lo}$ PBMCs from cancer patients, compared to healthy donors (Supplementary Fig.7). However, this population was significantly expanded from 0.5% of total PBMCs in healthy donors to up to 17% in cancer patients (Fig.7).

## Discussion

Using spontaneous genetic and syngeneic transplant tumor models, as well as an *ex vivo* differentiation model, we have established for the first time that tumor-derived signals drive expansion of monocytic MDSCs by inducing CD38 expression. Expansion of the $CD11b^{+}Gr1^{+}CD38^{high}$ cell population occurs after initial splenic MDSC accumulation is evident, which likely indicates a requirement of threshold levels of tumor-derived signals for induction of CD38 by MDSCs (Fig. 5D). Interestingly, two different ESCC cell lines exhibited differential capacities to induce expansion of $CD38^{high}$ MDSCs, thereby suggesting that the tumor cells are responsible for promoting CD38 expression on MDSCs. Based upon our *ex vivo* studies, the tumor-derived signals may act directly on immature myeloid cell populations present in hematopoietic tissues to promote CD38 expression. Furthermore, our data suggest that the tumor-derived signals do not promote enhanced proliferation of $CD38^{high}$ MDSCs (RB1 pathway was activated in $CD38^{high}$ MDSCs (Supplementary Fig. 5)), but provide these cells with increased survival potential.

Herein, we demonstrate that $CD38^{high}$ MDSCs are halted at an earlier differentiation stage compared to $CD38^{low}$ MDSCs. Binding of cognate ligand by CD38 can contribute directly to the differentiation halt (23), which suggests that CD38 signaling may contribute to the maintenance of undifferentiated state observed in $CD38^{high}$ MDSCs. Although CD38 has been demonstrated to bind CD31 (21), we do not know if this interaction contributes to the observed properties of $CD38^{high}$ MDSCs.

CD38$^{high}$ MDSCs express elevated iNOS levels compared to CD38$^{low}$ MDSCs, and iNOS is required for T cell suppression by CD38$^{high}$ MDSCs. Interestingly, CD38 can induce iNOS upregulation in murine activated microglia (resident monocytes of the brain) (35). Furthermore, *Cd38*$^{-/-}$ mice produce less tumor-associated microglia in a syngeneic transplant model of glioma (36). Strikingly, we have found that in *Cd38*$^{-/-}$ mice, subcutaneous ESCC tumors induce a less pronounced expansion of M-MDSCs, regardless of the cell line used to generate tumors (Supplementary Fig. 6). These findings support the premise that CD38 promotes expansion of M-MDSCs, as well as elevated iNOS expression. We also observed increased phospho-NFκB levels in CD11b$^{+}$Gr1$^{+}$CD38$^{high}$ cells. This is consistent with observations made in murine B cells, where CD38 ligation activates NFκB (37). Furthermore, NFκB-mediated activation of iNOS has been described in LPS-stimulated macrophages (38), highlighting the possibility that elevated phospho-NFκB levels in CD38$^{high}$ MDSCs may contribute to increased expression of iNOS observed in these cells.

Several factors are likely to be responsible for activating CD38 expression, including IFNγ, TNFα (34), as well as IL-6, IGFBP3 and CXCL16. We have demonstrated that IFNγ and TNFα induce bone marrow-derived CD11b$^{+}$Gr1$^{+}$ cells to express CD38 *ex vivo*. As both IFNγ and TNFα are often produced during chronic inflammation, they may be primary inducers of CD38 expression (Fig. 5D). In fact, TNFα inhibition can impair immunosuppressive capacity of MDSCs and induce differentiation in a murine model of chronic inflammation, while MDSCs from *Tnf*$^{-/-}$ mice have reduced iNOS levels (39).

Our finding of a CXCL16 and IGFBP-3-mediated response in MDSCs has not been described previously. However, CXCL16 expression can be promoted by IFNγ and TNFα (40), the two most potent inducers of CD38 expression in our *ex vivo* system. Interestingly, IGFBP-3 has been shown to increase intracellular $Ca^{2+}$ levels *in vitro* (41). $Ca^{2+}$ signaling, which can be mediated by ectoenzymatic activity of CD38 (34), is important for multiple immunomodulatory processes (42,43). Therefore, it is possible that in MDSCs IGFBP-3 can be modulating $Ca^{2+}$ mobilization by increasing CD38 expression.

IL-6 is a major regulator of STAT3 signaling, which is essential for establishment of immunosuppressive microenvironment within the tumor (44). In MDSCs, STAT3 activation enhances production of the S100A8/A9 pro-inflammatory proteins, which also contribute to maintenance of a low differentiation or immature state (45). These data are in agreement with our observation that IL-6 can promote CD38 expression on MDSCs generated *ex vivo*, since $CD38^{high}$ MDSCs are less differentiated than $CD38^{low}$ MDSCs (Fig. 4B).

Herein, we demonstrate the efficacy of anti-CD38 monoclonal antibody treatment *in vitro* and *in vivo*. Moreover, we report CD38 expression by human MDSCs; therefore, anti-CD38 therapy may represent a novel approach to targeting this immunosuppressive population in cancer treatment strategies. Furthermore, since $CD38^{high}$ Tregs possess enhanced suppressive potential compared to $CD38^{low}$ Tregs (18,19), anti-CD38 therapy may present the advantage of targeting several immunosuppressive cell types at the same time.

Recently, an anti-CD38 monoclonal antibody (Daratumumab) was shown to be efficient in treatment of multiple myeloma in pre-clinical studies (46). A similar approach may induce ablation of MDSCs in patients with advanced stage solid cancers, and thus, may be suitable as an adjuvant to conventional therapies. The expression pattern of CD38 in a broad range of cell types can raise a concern about potential adverse effects of anti-CD38 therapy (47), however, early clinical studies of Daratumumab in multiple myeloma have demonstrated an acceptable safety profile, suggesting that an appropriate dosage and treatment schedule allow for minimizing of the effects of targeting CD38 in normal tissue (48).

MDSCs contribute to the T cell suppression repertoire found in cancer, which merits further investigation as a prospective therapeutic target (49). In this study, we have identified CD38 as being suitable for potential MDSC targeting and useful in identification of potently immunosuppressive MDSC populations. Thus, anti-CD38 monoclonal antibody therapy (46) may hold potential for targeting CD38-expressing MDSCs (50) in patients with certain types of cancer.

## Acknowledgements

We are grateful to the Center for Molecular Studies in Digestive and Liver Diseases (NIH P30-DK050306), the Molecular Pathology and Imaging Core (J. Katz, A. Bedenbaugh, D. Budo, and R. Hasan), the Molecular Biology/Gene Expression Core (G. Wu and S. Keilbaugh), the Transgenic and Chimeric Mouse Core, the Penn Microarray and Flow Cytometry and Cell Sorting Facilities. We also thank Ann Tierney for assistance with statistical analyses and to members of the Rustgi and Singhal laboratories for discussions.

## References

1. Schreiber RD, Old LJ, Smyth MJ. Cancer immunoediting: integrating immunity's roles in cancer suppression and promotion. Science [Internet]. 2011 [cited 2014 Jul 10];331:1565–70. Available from: http://www.ncbi.nlm.nih.gov/pubmed/21436444

2. Waldron, T J, Quatromoni G J, Karakasheva, T A, Singhal, S, Rustgi AK. Myeloid derived suppressor cells: Targets for therapy. Oncoimmunology [Internet]. Landes Bioscience; 2013 [cited 2013 May 1];2:e24117. Available from: http://www.landesbioscience.com/journals/oncoimmunology/article/24117/

3. Gabrilovich DI, Nagaraj S. Myeloid-derived suppressor cells as regulators of the immune system. Nat Rev Immunol [Internet]. 2009/02/07 ed. 2009;9:162–74. Available from: http://www.ncbi.nlm.nih.gov/pubmed/19197294

4. Pak AS, Wright MA, Matthews JP, Collins SL, Petruzzelli GJ, Young MR. Mechanisms of immune suppression in patients with head and neck cancer: presence of CD34(+) cells which suppress immune functions within cancers that secrete granulocyte-macrophage colony-stimulating factor. Clin Cancer Res [Internet]. 1995 [cited 2014 Oct 20];1:95–103. Available from: http://www.ncbi.nlm.nih.gov/pubmed/9815891

5. Gabitass RF, Annels NE, Stocken DD, Pandha HA, Middleton GW. Elevated myeloid-derived suppressor cells in pancreatic, esophageal and gastric cancer are an independent prognostic factor and are associated with significant elevation of the Th2 cytokine interleukin-13. Cancer Immunol Immunother [Internet]. 2011 [cited 2014 May 20];60:1419–30. Available from: http://www.pubmedcentral.nih.gov/articlerender.fcgi?artid=3176406&tool=pmcentrez&rendertype=abstract

6. Schmielau J, Finn OJ. Activated granulocytes and granulocyte-derived hydrogen peroxide are the underlying mechanism of suppression of t-cell function in advanced cancer patients. Cancer Res [Internet]. 2001 [cited 2014 Oct 20];61:4756–60. Available from: http://www.ncbi.nlm.nih.gov/pubmed/11406548

7. Liu C-Y, Wang Y-M, Wang C-L, Feng P-H, Ko H-W, Liu Y-H, et al. Population alterations of L-arginase- and inducible nitric oxide synthase-expressed CD11b+/CD14$^-$/CD15+/CD33+ myeloid-derived suppressor cells and CD8+ T lymphocytes in patients with advanced-stage non-small cell lung cancer. J Cancer Res Clin Oncol [Internet]. 2010 [cited 2014 Oct 20];136:35–45. Available from: http://www.ncbi.nlm.nih.gov/pubmed/19572148

8. Zea AH, Rodriguez PC, Atkins MB, Hernandez C, Signoretti S, Zabaleta J, et al. Arginase-producing myeloid suppressor cells in renal cell carcinoma

patients: a mechanism of tumor evasion. Cancer Res [Internet]. 2005 [cited 2014 Oct 20];65:3044–8. Available from: http://www.ncbi.nlm.nih.gov/pubmed/15833831

9. Filipazzi P, Valenti R, Huber V, Pilla L, Canese P, Iero M, et al. Identification of a new subset of myeloid suppressor cells in peripheral blood of melanoma patients with modulation by a granulocyte-macrophage colony-stimulation factor-based antitumor vaccine. J Clin Oncol [Internet]. 2007 [cited 2012 Nov 4];25:2546–53. Available from: http://www.ncbi.nlm.nih.gov/pubmed/17577033

10. Vuk-Pavlović S, Bulur PA, Lin Y, Qin R, Szumlanski CL, Zhao X, et al. Immunosuppressive CD14+HLA-DRlow/- monocytes in prostate cancer. Prostate [Internet]. 2010 [cited 2014 Oct 20];70:443–55. Available from: http://www.pubmedcentral.nih.gov/articlerender.fcgi?artid=2935631&tool=pmcentrez&rendertype=abstract

11. Greten TF, Manns MP, Korangy F. Myeloid derived suppressor cells in human diseases. Int Immunopharmacol [Internet]. 2011 [cited 2013 Nov 6];11:802–7. Available from: http://www.pubmedcentral.nih.gov/articlerender.fcgi?artid=3478130&tool=pmcentrez&rendertype=abstract

12. Li H, Han Y, Guo Q, Zhang M, Cao X. Cancer-expanded myeloid-derived suppressor cells induce anergy of NK cells through membrane-bound TGF-

beta 1. J Immunol [Internet]. 2009 [cited 2014 Oct 20];182:240–9. Available from: http://www.ncbi.nlm.nih.gov/pubmed/19109155

13. Huang B, Pan P-Y, Li Q, Sato AI, Levy DE, Bromberg J, et al. Gr-1+CD115+ immature myeloid suppressor cells mediate the development of tumor-induced T regulatory cells and T-cell anergy in tumor-bearing host. Cancer Res [Internet]. 2006 [cited 2014 Sep 12];66:1123–31. Available from: http://www.ncbi.nlm.nih.gov/pubmed/16424049

14. Rodriguez PC, Zea AH, DeSalvo J, Culotta KS, Zabaleta J, Quiceno DG, et al. L-arginine consumption by macrophages modulates the expression of CD3 zeta chain in T lymphocytes. J Immunol [Internet]. 2003 [cited 2014 Oct 20];171:1232–9. Available from: http://www.ncbi.nlm.nih.gov/pubmed/12874210

15. Bingisser RM, Tilbrook PA, Holt PG, Kees UR. Macrophage-derived nitric oxide regulates T cell activation via reversible disruption of the Jak3/STAT5 signaling pathway. J Immunol [Internet]. 1998 [cited 2014 Oct 20];160:5729–34. Available from: http://www.ncbi.nlm.nih.gov/pubmed/9637481

16. Harari O, Liao JK. Inhibition of MHC II gene transcription by nitric oxide and antioxidants. Curr Pharm Des [Internet]. 2004 [cited 2014 Oct 20];10:893–8. Available from:

http://www.pubmedcentral.nih.gov/articlerender.fcgi?artid=2633593&tool=pmcentrez&rendertype=abstract

17. Rivoltini L, Carrabba M, Huber V, Castelli C, Novellino L, Dalerba P, et al. Immunity to cancer: attack and escape in T lymphocyte-tumor cell interaction. Immunol Rev [Internet]. 2002 [cited 2014 Oct 20];188:97–113. Available from: http://www.ncbi.nlm.nih.gov/pubmed/12445284

18. Patton DT, Wilson MD, Rowan WC, Soond DR, Okkenhaug K. The PI3K p110δ regulates expression of CD38 on regulatory T cells. PLoS One [Internet]. 2011 [cited 2014 Oct 20];6:e17359. Available from: http://www.pubmedcentral.nih.gov/articlerender.fcgi?artid=3046981&tool=pmcentrez&rendertype=abstract

19. Bahri R, Bollinger A, Bollinger T, Orinska Z, Bulfone-Paus S. Ectonucleotidase CD38 demarcates regulatory, memory-like CD8+ T cells with IFN-γ-mediated suppressor activities. PLoS One [Internet]. 2012 [cited 2014 Oct 9];7:e45234. Available from: http://www.pubmedcentral.nih.gov/articlerender.fcgi?artid=3444472&tool=pmcentrez&rendertype=abstract

20. Blair PA, Noreña LY, Flores-Borja F, Rawlings DJ, Isenberg DA, Ehrenstein MR, et al. CD19(+)CD24(hi)CD38(hi) B cells exhibit regulatory capacity in healthy individuals but are functionally impaired in systemic Lupus Erythematosus patients. Immunity [Internet]. 2010 [cited 2014 Oct

20];32:129–40. Available from: http://www.ncbi.nlm.nih.gov/pubmed/20079667

21. Malavasi F, Deaglio S, Funaro A, Ferrero E, Horenstein AL, Ortolan E, et al. Evolution and function of the ADP ribosyl cyclase/CD38 gene family in physiology and pathology. Physiol Rev. 2008;88:841–86.

22. Lee HC. Cyclic ADP-ribose and nicotinic acid adenine dinucleotide phosphate (NAADP) as messengers for calcium mobilization. J Biol Chem [Internet]. 2012 [cited 2014 Jul 21];287:31633–40. Available from: http://www.jbc.org/content/287/38/31633.short

23. Todisco E, Suzuki T, Srivannaboon K, Coustan-Smith E, Raimondi SC, Behm FG, et al. CD38 ligation inhibits normal and leukemic myelopoiesis. Blood [Internet]. 2000/01/11 ed. 2000;95:535–42. Available from: http://www.ncbi.nlm.nih.gov/pubmed/10627459

24. Stairs DB, Bayne LJ, Rhoades B, Vega ME, Waldron TJ, Kalabis J, et al. Deletion of p120-catenin results in a tumor microenvironment with inflammation and cancer that establishes it as a tumor suppressor gene. Cancer Cell [Internet]. 2011/04/13 ed. 2011;19:470–83. Available from: http://www.ncbi.nlm.nih.gov/pubmed/21481789

25. Youn J-I, Nagaraj S, Collazo M, Gabrilovich DI. Subsets of myeloid-derived suppressor cells in tumor-bearing mice. J Immunol [Internet]. 2008 [cited 2013 Jan 28];181:5791–802. Available from:

http://www.pubmedcentral.nih.gov/articlerender.fcgi?artid=2575748&tool=pmcentrez&rendertype=abstract

26. Partida-Sánchez S, Cockayne DA, Monard S, Jacobson EL, Oppenheimer N, Garvy B, et al. Cyclic ADP-ribose production by CD38 regulates intracellular calcium release, extracellular calcium influx and chemotaxis in neutrophils and is required for bacterial clearance in vivo. Nat Med [Internet]. 2001 [cited 2013 Jan 16];7:1209–16. Available from: http://www.ncbi.nlm.nih.gov/pubmed/11689885

27. Partida-Sanchez S, Iribarren P, Moreno-Garcia ME, Gao J-L, Murphy PM, Oppenheimer N, et al. Chemotaxis and Calcium Responses of Phagocytes to Formyl Peptide Receptor Ligands Is Differentially Regulated by Cyclic ADP Ribose. J Immunol [Internet]. 2004 [cited 2014 Sep 11];172:1896–906. Available from: http://www.jimmunol.org/cgi/doi/10.4049/jimmunol.172.3.1896

28. Malavasi F, Deaglio S, Damle R, Cutrona G, Ferrarini M, Chiorazzi N. CD38 and chronic lymphocytic leukemia: a decade later. Blood [Internet]. 2011/07/19 ed. 2011;118:3470–8. Available from: http://www.ncbi.nlm.nih.gov/pubmed/21765022

29. Quante M, Bhagat G, Abrams J a, Marache F, Good P, Lee MD, et al. Bile acid and inflammation activate gastric cardia stem cells in a mouse model of Barrett-like metaplasia. Cancer Cell [Internet]. Elsevier Inc.; 2012 [cited

2012 Jul 12];21:36–51. Available from: http://www.ncbi.nlm.nih.gov/pubmed/22264787

30. Opitz O, Harada H. A mouse model of human oral-esophageal cancer. J … [Internet]. 2002 [cited 2014 Oct 20];110:761–9. Available from: http://www.jci.org/articles/view/15324

31. Takaoka M, Harada H, Deramaudt TB, Oyama K, Andl CD, Johnstone CN, et al. Ha-Ras(G12V) induces senescence in primary and immortalized human esophageal keratinocytes with p53 dysfunction. Oncogene [Internet]. Nature Publishing Group; 2004 [cited 2013 Apr 11];23:6760–8. Available from: http://dx.doi.org/10.1038/sj.onc.1207923

32. Aktan F. iNOS-mediated nitric oxide production and its regulation. Life Sci [Internet]. 2004 [cited 2014 Oct 13];75:639–53. Available from: http://www.ncbi.nlm.nih.gov/pubmed/15172174

33. Muller-Steffner HM, Malver O, Hosie L, Oppenheimer NJ, Schuber F. Slow-binding inhibition of NAD+ glycohydrolase by arabino analogues of beta-NAD. J Biol Chem [Internet]. 1992 [cited 2014 Oct 21];267:9606–11. Available from: http://www.ncbi.nlm.nih.gov/pubmed/1315761

34. Malavasi F, Deaglio S, Funaro A, Ferrero E, Horenstein AL, Ortolan E, et al. Evolution and function of the ADP ribosyl cyclase/CD38 gene family in physiology and pathology. Physiol Rev [Internet]. 2008/07/16 ed.

2008;88:841–86. Available from: http://www.ncbi.nlm.nih.gov/pubmed/18626062

35. Mayo L, Jacob-Hirsch J, Amariglio N, Rechavi G, Moutin M-J, Lund FE, et al. Dual Role of CD38 in Microglial Activation and Activation-Induced Cell Death. J Immunol [Internet]. 2008 [cited 2014 Sep 11];181:92–103. Available from: http://www.jimmunol.org/cgi/doi/10.4049/jimmunol.181.1.92

36. Levy A, Blacher E, Vaknine H, Lund FE, Stein R, Mayo L. CD38 deficiency in the tumor microenvironment attenuates glioma progression and modulates features of tumor-associated microglia/macrophages. Neuro Oncol [Internet]. 2012 [cited 2013 Sep 19];14:1037–49. Available from: http://www.pubmedcentral.nih.gov/articlerender.fcgi?artid=3408254&tool=pmcentrez&rendertype=abstract

37. Kaku H, Horikawa K, Obata Y, Kato I, Okamoto H, Sakaguchi N, et al. NF-kappaB is required for CD38-mediated induction of C(gamma)1 germline transcripts in murine B lymphocytes. Int Immunol [Internet]. 2002 [cited 2014 Oct 20];14:1055–64. Available from: http://www.ncbi.nlm.nih.gov/pubmed/12202402

38. Xie QW, Kashiwabara Y, Nathan C. Role of transcription factor NF-kappa B/Rel in induction of nitric oxide synthase. J Biol Chem [Internet]. 1994 [cited 2014 Oct 20];269:4705–8. Available from: http://www.ncbi.nlm.nih.gov/pubmed/7508926

39. Sade-Feldman M, Kanterman J, Ish-Shalom E, Elnekave M, Horwitz E, Baniyash M. Tumor necrosis factor-α blocks differentiation and enhances suppressive activity of immature myeloid cells during chronic inflammation. Immunity [Internet]. 2013 [cited 2014 Oct 20];38:541–54. Available from: http://www.ncbi.nlm.nih.gov/pubmed/23477736

40. Abel S, Hundhausen C, Mentlein R, Schulte A, Berkhout TA, Broadway N, et al. The transmembrane CXC-chemokine ligand 16 is induced by IFN-gamma and TNF-alpha and shed by the activity of the disintegrin-like metalloproteinase ADAM10. J Immunol [Internet]. 2004 [cited 2014 Oct 20];172:6362–72. Available from: http://www.ncbi.nlm.nih.gov/pubmed/15128827

41. Seurin D, Lombet A, Babajko S, Godeau F, Ricort J-M. Insulin-like growth factor binding proteins increase intracellular calcium levels in two different cell lines. PLoS One [Internet]. 2013 [cited 2013 Jun 7];8:e59323. Available from: http://www.pubmedcentral.nih.gov/articlerender.fcgi?artid=3602172&tool=pmcentrez&rendertype=abstract

42. Sochorová K, Budinský V, Rozková D, Tobiasová Z, Dusilová-Sulková S, Spísek R, et al. Paricalcitol (19-nor-1,25-dihydroxyvitamin D2) and calcitriol (1,25-dihydroxyvitamin D3) exert potent immunomodulatory effects on dendritic cells and inhibit induction of antigen-specific T cells. Clin Immunol

[Internet]. 2009 [cited 2013 Jun 7];133:69–77. Available from: http://www.ncbi.nlm.nih.gov/pubmed/19660988

43. Vukcevic M, Zorzato F, Spagnoli G, Treves S. Frequent calcium oscillations lead to NFAT activation in human immature dendritic cells. J Biol Chem [Internet]. 2010 [cited 2013 Jun 7];285:16003–11. Available from: http://www.pubmedcentral.nih.gov/articlerender.fcgi?artid=2871469&tool=pmcentrez&rendertype=abstract

44. Kortylewski M, Kujawski M, Wang T, Wei S, Zhang S, Pilon-Thomas S, et al. Inhibiting Stat3 signaling in the hematopoietic system elicits multicomponent antitumor immunity. Nat Med [Internet]. 2005 [cited 2013 May 26];11:1314–21. Available from: http://www.ncbi.nlm.nih.gov/pubmed/16288283

45. Sinha P, Okoro C, Foell D, Freeze HH, Ostrand-Rosenberg S, Srikrishna G. Proinflammatory S100 proteins regulate the accumulation of myeloid-derived suppressor cells. J Immunol [Internet]. 2008 [cited 2012 Nov 19];181:4666–75. Available from: http://www.pubmedcentral.nih.gov/articlerender.fcgi?artid=2810501&tool=pmcentrez&rendertype=abstract

46. De Weers M, Tai Y-T, van der Veer MS, Bakker JM, Vink T, Jacobs DCH, et al. Daratumumab, a novel therapeutic human CD38 monoclonal

antibody, induces killing of multiple myeloma and other hematological tumors. J Immunol [Internet]. 2011 [cited 2014 Sep 25];186:1840–8. Available from: http://www.ncbi.nlm.nih.gov/pubmed/21187443

47. Stevenson GT. CD38 as a therapeutic target. Mol Med [Internet]. 2007/03/24 ed. 2006;12:345–6. Available from: http://www.ncbi.nlm.nih.gov/pubmed/17380203

48. Laubach JP, Tai Y-T, Richardson PG, Anderson KC. Daratumumab granted breakthrough drug status. Expert Opin Investig Drugs [Internet]. 2014 [cited 2014 Oct 27];23:445–52. Available from: http://www.ncbi.nlm.nih.gov/pubmed/24555809

49. Marigo I, Dolcetti L, Serafini P, Zanovello P, Bronte V. Tumor-induced tolerance and immune suppression by myeloid derived suppressor cells. Immunol Rev [Internet]. 2008 [cited 2014 Oct 20];222:162–79. Available from: http://www.ncbi.nlm.nih.gov/pubmed/18364001

50. Chillemi A, Zaccarello G, Quarona V, Ferracin M, Ghimenti C, Massaia M, et al. Anti-CD38 antibody therapy: windows of opportunity yielded by the functional characteristics of the target molecule. Mol Med [Internet]. 2013 [cited 2014 Oct 20];19:99–108. Available from: http://www.pubmedcentral.nih.gov/articlerender.fcgi?artid=3667209&tool=pmcentrez&rendertype=abstract

**Figure 1. CD38 is significantly upregulated in CD11b$^{+}$Gr1$^{+}$ cells from tumor-bearing *p120$^{-/-}$* mice.** (A) Heatmap illustrating the results of a microarray analysis performed using CD11b$^{+}$Gr1$^{+}$ cells sorted from the spleens of 6 tumor-bearing *p120$^{-/-}$* mice and 3 pooled samples from healthy littermate controls (n=9). Increased expression of the *Cd38* gene and protein in CD11b$^{+}$Gr1$^{+}$ cells from tumor-bearing mice was confirmed by (B) qPCR (*p=0.007) and (C) FACS (n= 3; *p=0.009). (D) Frequencies of CD38$^{+}$ cells (*p=0.003).

**Figure 2. CD38 expression increases in monocytic myeloid cells with disease progression.** (A) Splenocytes from healthy control, non-diseased (ND) *p120$^{-/-}$* and tumor-bearing (TB) *p120$^{-/-}$* mice were analyzed by FACS for CD38 expression on myeloid cell populations. (B) Histograms comparing CD38-FITC fluorescence levels on two cell subsets from control, *p120$^{-/-}$* non-diseased and *p120$^{-/-}$* tumor-bearing mice. (C) Splenocytes from control non-diseased and AKR or HNM007 subcutaneous tumor-bearing C57BL/6 mice analyzed by FACS. Histograms compare CD38 expression levels in listed subpopulations from control and tumor-bearing mice. (D) Splenocytes from control and tumor-bearing mice were analyzed by FACS for distribution of CD11b, Ly6C, Ly6G and CD38 antigens. Pie charts demonstrate the frequencies of lymphoid (CD11b$^{-}$) and myeloid (CD11b$^{+}$) cell populations in spleens of control and tumor-bearing mice with the myeloid population further broken down into Ly6C$^{+}$, Ly6G$^{+}$ and Ly6C$^{-}$ Ly6G$^{-}$ subsets (n=3 per group).

**Figure 3. CD38$^{High}$ MDSCs are more immunosuppressive and promote tumor growth more efficiently than the CD38$^{Low}$ MDSCs.** (A) CD38$^{high}$ and CD38$^{low}$ MDSCs from tumor-bearing *p120*$^{-/-}$ mice were used in a T cell suppression assay (n=3; *p=0.0007). (B) C57BL/6 mice were injected with HNM007 cells in combination with MDSCs (CD38$^{High}$ or CD38$^{Low}$) or alone (n=5 per group). Tumor volumes were compared between the CD38$^{High}$ and CD38$^{Low}$ groups (*p=0.004 and 0.03), and between CD38$^{High}$ and control HNM007 tumors (** p=0.01, 0.003 and 0.01). (C) Representative H&E and CD45 immunohistochemistry of CD38$^{High}$-injected, CD38$^{Low}$ or control tumors. (D) Tumors were scored for abundance of necrotic areas and inflammatory infiltrate on the scale 0-4. (E) Splenic MDSCs from HNM007 tumor-bearing *Cd38-/-* or *wt* mice were used in a T cell suppression assay (*p=0.003 and 0.04).

**Figure 4. CD38$^{High}$ MDSCs are phenotypically different from the CD38$^{Low}$ subset.** (A) Heatmap illustrating the results of a microarray analysis performed using CD38$^{High}$ and CD38$^{Low}$ CD11b$^{+}$Gr1$^{+}$ cells sorted from spleens of 4 tumor-bearing *p120*$^{-/-}$ mice. (B) qPCR analysis of *iNos*, *Arg1* and *Nox2* gene expression (*p=9x10$^{-8}$). (C) Western blot analysis of iNOS and phospho-NFκB protein levels in CD38$^{High}$ and CD38$^{Low}$ MDSCs. (D) iNOS inhibitor (L-NMMA) and (E)CD38 inhibitor (AraF-NAD) were tested in a T cell suppression assay (*p=0.004 and 0.04, respectively). (F) Expression levels of iNOS in splenic MDSCs from tumor-bearing *Cd38-/-* or *wt* mice were assessed by FACS. (G) Cytospin preparations from CD38$^{high}$ and CD38$^{Low}$ MDSCs.

**Figure 5. IFNγ, TNFα, IGFBP-3, CXCL16 and IL-6 induce CD38 expression and impair myeloid cell differentiation**. (A) CD38 expression in CD11b$^+$Gr1$^+$ cells from *ex vivo* differentiation cultures was tested by FACS. Results are presented as mean fluorescence intensity (MFI) (n=3; * $p \leq 0.0001$, **$p=2.5 \times 10^{-5}$). (B) Cytokine array performed with media from *ex vivo* differentiation cultures (24 or 120-hour). Each cytokine tested in duplicate. Difference in normalized expression between HNM007 and AKR groups is shown. (C) *Ex vivo* differentiation as in (A) with the addition of cytokines to the AKR conditioned media (n=3; *$p<0.05$, ** $p<0.005$). (E) In mice, early stages of cancer initiation and progression lead to MDSC expansion. Tumor progression leads to amplified signals (such as cytokines) reaching MDSCs, which induces a differentiation halt and expansion of CD38$^{High}$ monocytic MDSCs with enhanced immunosuppressive capacity (mediated by iNOS, which produces nitric oxide (NO)).

**Figure 6. Cross-linking of CD38 by an agonistic antibody impairs expansion and survival of CD11b$^+$Gr1$^+$ cells *in vitro* and suppresses tumor growth *in vivo*.** (A) Representative images from methylcellulose cultures of CD11b$^+$Gr1$^+$ cells treated with anti-CD38 monoclonal antibody (NIMR-5) or isotype control (IgG2a), after 5 days of culture. (B) Number of colonies formed following 7 days of culture (n=3; *$p=4 \times 10^{-5}$). (C) CD11b$^+$Gr1$^+$ cells were cultured in RPMI with anti-CD38 or isotype control antibody, and counted at indicated time points. (n=6

per group; $*p<5x10^{-7}$, $**p<2x10^{-7}$, $***p<0.0005$). (D) *Ex vivo* differentiation performed with HNM007 conditioned medium and anti-CD38 agonist (NIM-R5) or isotype control (IgG2a) antibody. CD38 expression (using the clone 90 antibody) on the surface of $CD45^+7\text{-}AAD^-CD11b^+Gr1^+$ was measured by FACS (n=3 per group; * $p<0.003$, ** $p<0.0005$). (E) HNM007 tumor growth kinetics in C57BL/6 mice treated with anti-CD38 (NIM-R5) or isotype control (IgG2a) antibody (start of treatment is marked by an arrow, n=6 per group; *p=0.005, 0.005 and 0.04).

**Figure 7. $CD38^+$ MDSC-like population is expanded in the peripheral blood of advanced-stage cancer patients.** Histograms depict frequencies of $CD38^+CD15^{high}CD33^{low}$ cells in peripheral blood mononuclear cells (PBMC) from head and neck (HNC) and non-small cell lung (NSCLC) cancer patients and healthy donors.

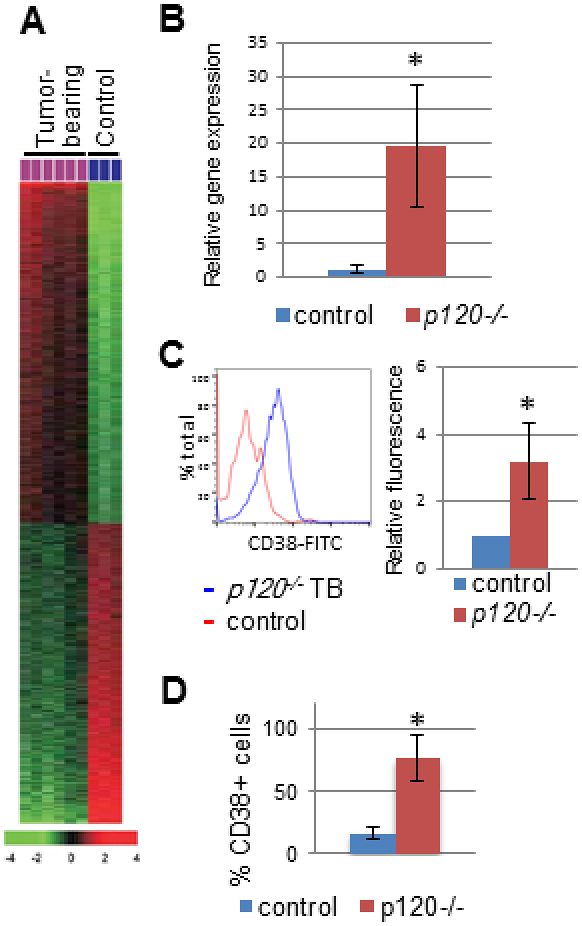
A
Tumor-bearing
Control
-4
-2
0
2
4
B
Relative gene expression
35
30
25
20
15
10
5
0
*
control
p120-/-
C
% total
CD38-FITC
p120-/- TB
control
Relative fluorescence
6
4
2
0
*
control
p120-/-
D
% CD38+ cells
100
50
0
*
control
p120-/-

**Figure 1**

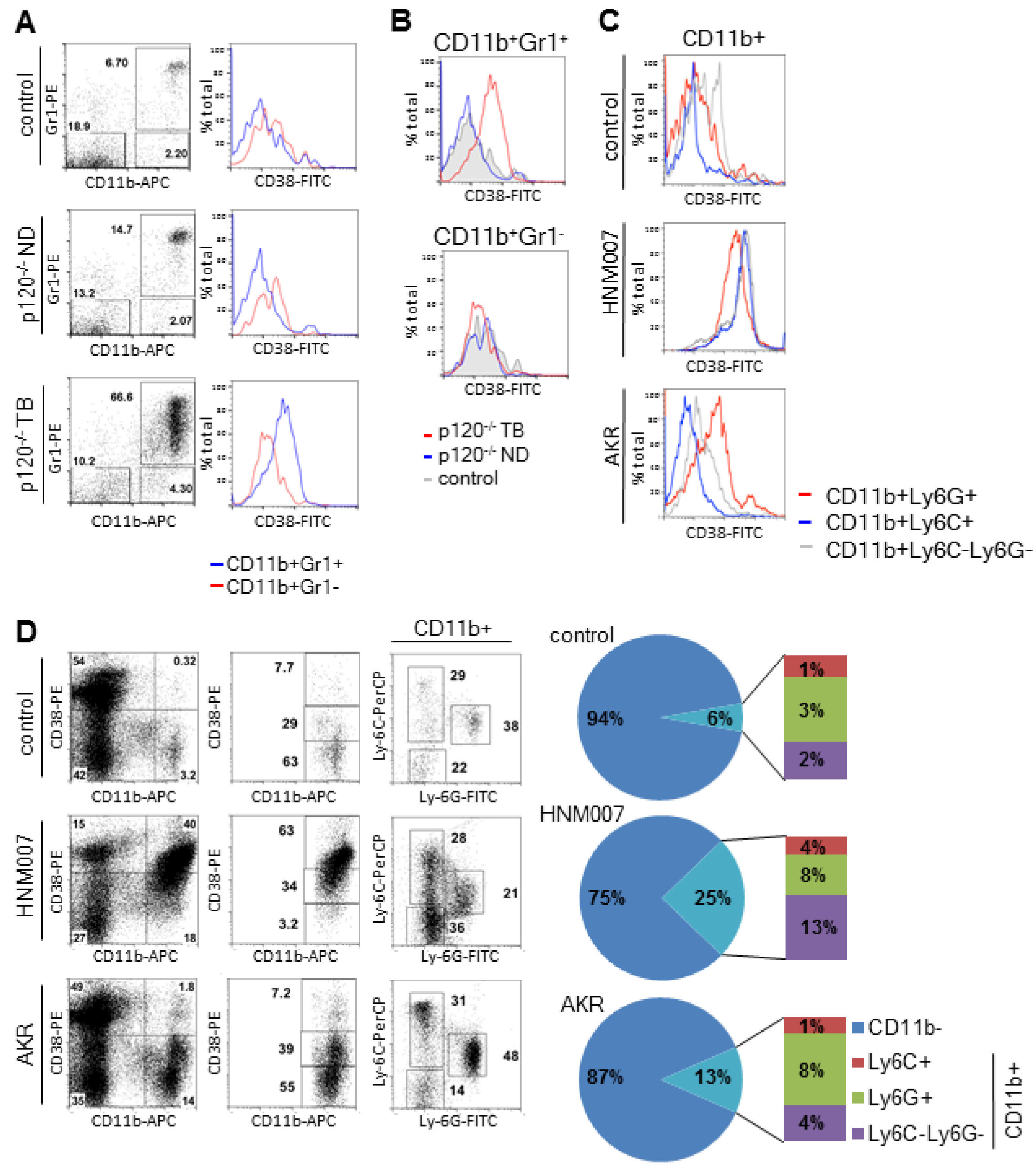
A
control
p120-/- ND
p120-/- TB
Gr1-PE
CD11b-APC
% total
CD38-FITC
6.70
18.9
2.20
14.7
13.2
2.07
66.6
10.2
4.30
CD11b+Gr1+
CD11b+Gr1-
B
CD11b+Gr1+
CD11b+Gr1-
p120-/- TB
p120-/- ND
control
C
CD11b+
control
HNM007
AKR
CD11b+Ly6G+
CD11b+Ly6C+
CD11b+Ly6C-Ly6G-
D
CD11b+
CD38-PE
Ly-6C-PerCP
Ly-6G-FITC
54
0.32
42
3.2
7.7
29
63
29
38
22
15
40
27
18
63
34
3.2
28
21
36
49
1.8
35
14
7.2
39
55
31
48
14
94%
6%
1%
3%
2%
75%
25%
4%
8%
13%
87%
13%
1%
8%
4%
CD11b-
Ly6C+
Ly6G+
Ly6C-Ly6G-
CD11b+

**Figure 2**

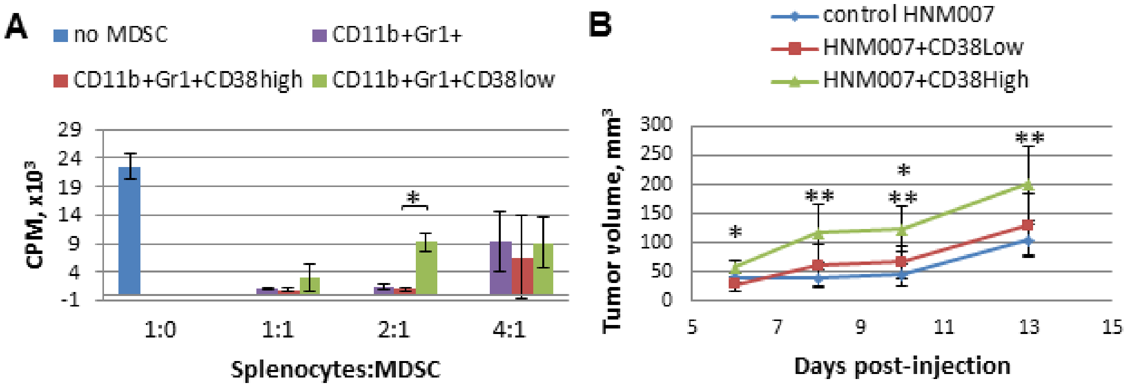

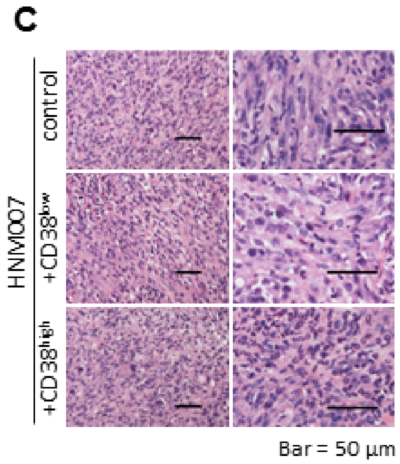

**D**

| group | sample # | inflammatory infiltrate |  |  |  | necrosis |  |  |  |
|---|---|---|---|---|---|---|---|---|---|
|  |  | score | mean | stdev | p | score | mean | stdev | p |
| control HNM007 | 1 | 2 | 1.4 | 0.55 |  | 0 | 0.6 | 0.89 |  |
|  | 2 | 1 |  |  |  | 1 |  |  |  |
|  | 3 | 1 |  |  |  | 2 |  |  |  |
|  | 4 | 1 |  |  |  | 0 |  |  |  |
|  | 5 | 2 |  |  |  | 0 |  |  |  |
| HNM007 +CD38$^{low}$ | 1 | 2 | 2.4 | 0.89 | 0.066 | 2 | 2 | 1.41 | 0.098 |
|  | 2 | 2 |  |  |  | 2 |  |  |  |
|  | 3 | 2 |  |  |  | 4 |  |  |  |
|  | 4 | 2 |  |  |  | 2 |  |  |  |
|  | 5 | 4 |  |  |  | 0 |  |  |  |
| HNM007 +CD38$^{high}$ | 1 | 4 | 3.6 | 0.89 | 0.002 | 4 | 3 | 1.41 | 0.013 |
|  | 2 | 4 |  |  |  | 1 |  |  |  |
|  | 3 | 4 |  |  |  | 2 |  |  |  |
|  | 4 | 4 |  |  |  | 4 |  |  |  |
|  | 5 | 2 |  |  |  | 4 |  |  |  |

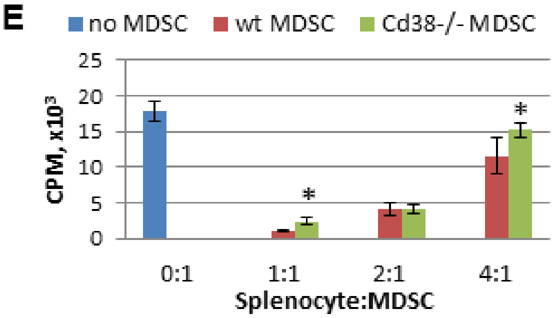

Figure 3

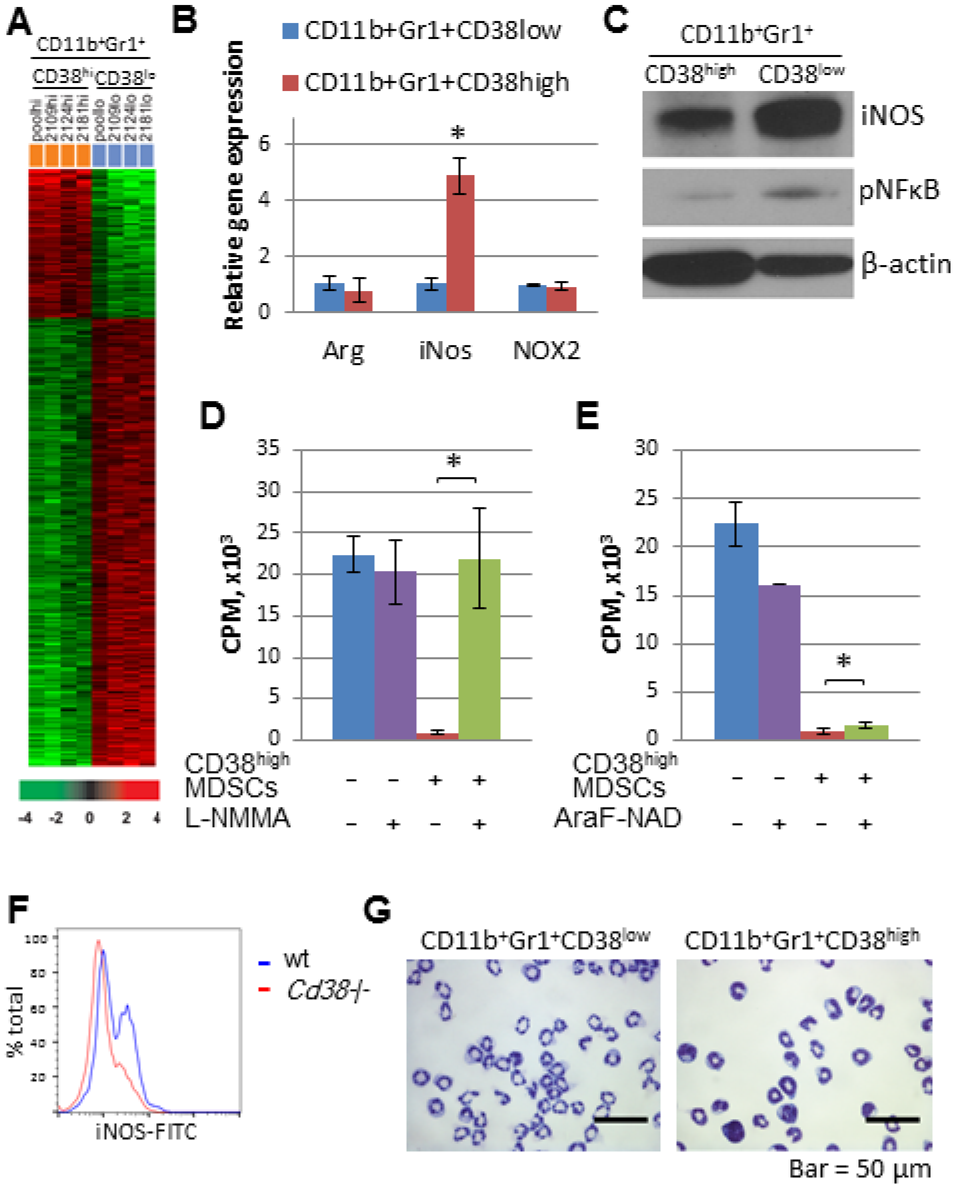
A
CD11b⁺Gr1⁺
CD38ʰⁱ
CD38ˡᵒ
poolhi
2109hi
2124hi
2181hi
poollo
2109lo
2124lo
2181lo
-4
-2
0
2
4
B
CD11b+Gr1+CD38low
CD11b+Gr1+CD38high
Relative gene expression
0
2
4
6
*
Arg
iNos
NOX2
C
CD11b⁺Gr1⁺
CD38ʰⁱᵍʰ
CD38ˡᵒʷ
iNOS
pNFκB
β-actin
D
CPM, x10³
0
5
10
15
20
25
30
35
*
CD38ʰⁱᵍʰ MDSCs
– – + +
L-NMMA
– + – +
E
CPM, x10³
0
5
10
15
20
25
30
*
CD38ʰⁱᵍʰ MDSCs
– – + +
AraF-NAD
– + – +
F
% total
20
40
60
80
100
iNOS-FITC
wt
Cd38-/-
G
CD11b⁺Gr1⁺CD38ˡᵒʷ
CD11b⁺Gr1⁺CD38ʰⁱᵍʰ
Bar = 50 µm

**Figure 4**

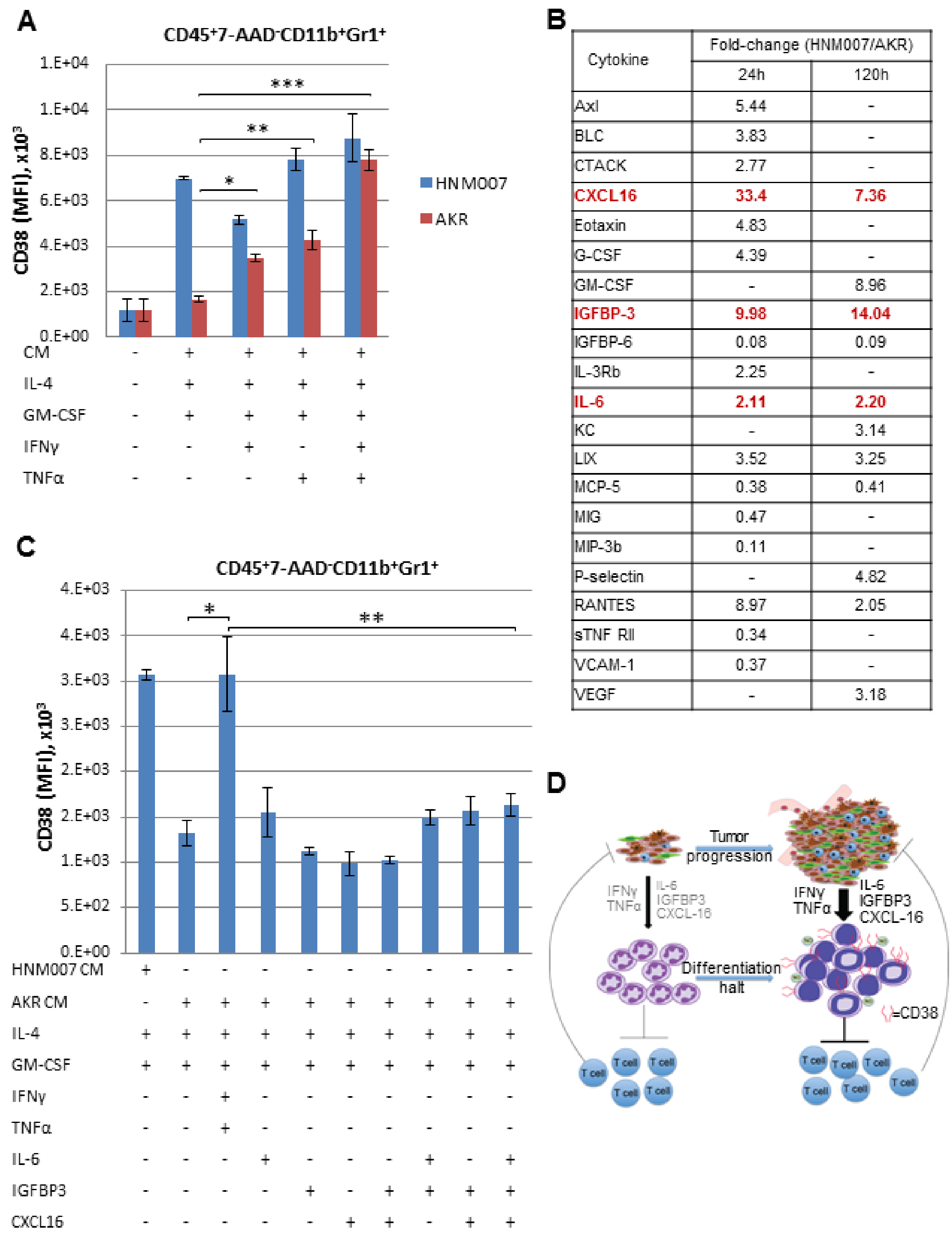

| Cytokine | Fold-change (HNM007/AKR) | |
|---|---|---|
| | 24h | 120h |
| Axl | 5.44 | - |
| BLC | 3.83 | - |
| CTACK | 2.77 | - |
| CXCL16 | 33.4 | 7.36 |
| Eotaxin | 4.83 | - |
| G-CSF | 4.39 | - |
| GM-CSF | - | 8.96 |
| IGFBP-3 | 9.98 | 14.04 |
| IGFBP-6 | 0.08 | 0.09 |
| IL-3Rb | 2.25 | - |
| IL-6 | 2.11 | 2.20 |
| KC | - | 3.14 |
| LIX | 3.52 | 3.25 |
| MCP-5 | 0.38 | 0.41 |
| MIG | 0.47 | - |
| MIP-3b | 0.11 | - |
| P-selectin | - | 4.82 |
| RANTES | 8.97 | 2.05 |
| sTNF RII | 0.34 | - |
| VCAM-1 | 0.37 | - |
| VEGF | - | 3.18 |

**Figure 5**

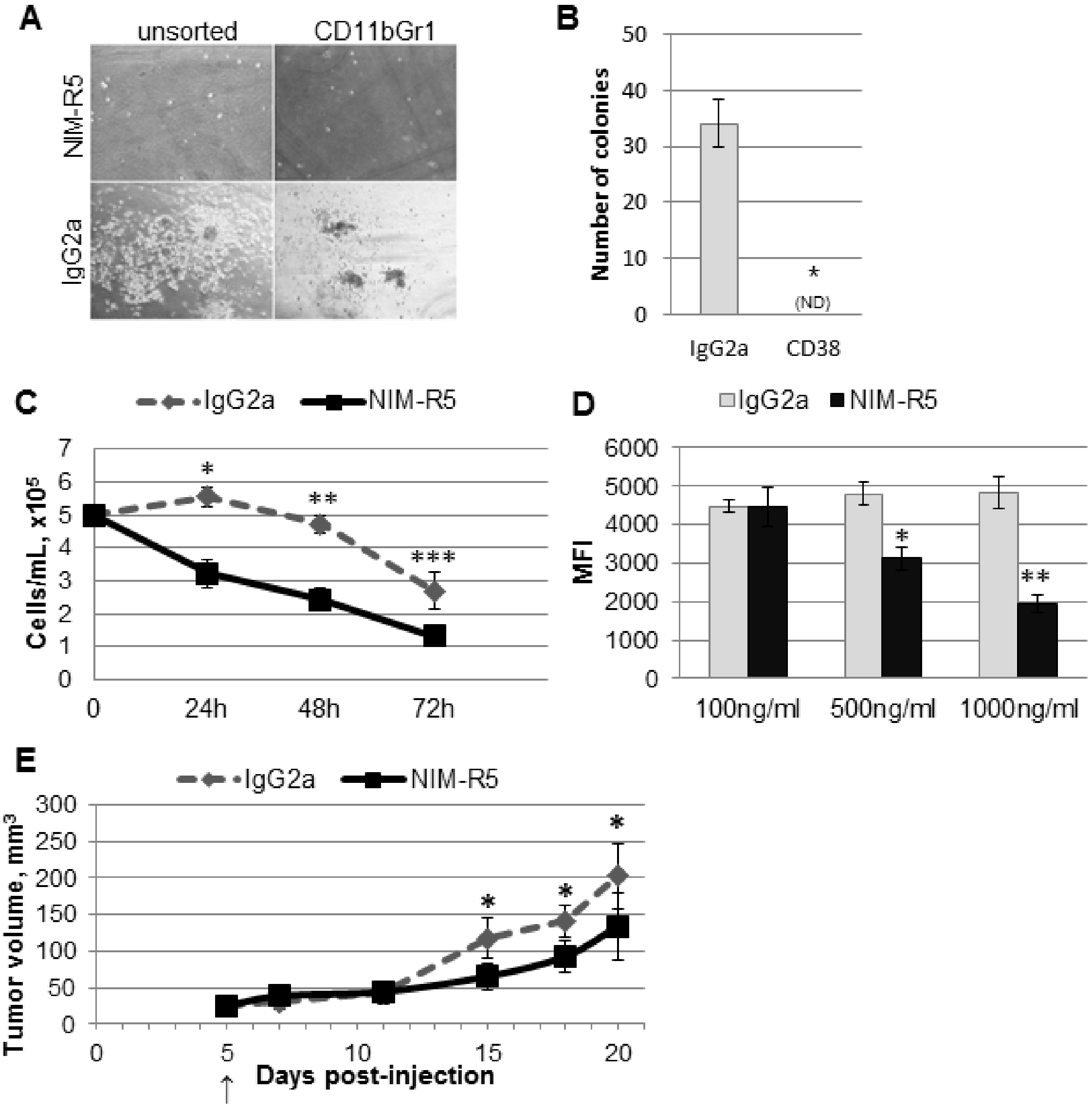
A
unsorted
CD11bGr1
NIM-R5
IgG2a
B
Number of colonies
50
40
30
20
10
0
*
(ND)
IgG2a
CD38
C
IgG2a
NIM-R5
Cells/mL, x10$^5$
7
6
5
4
3
2
1
0
*
**
***
0
24h
48h
72h
D
IgG2a
NIM-R5
MFI
6000
5000
4000
3000
2000
1000
0
*
**
100ng/ml
500ng/ml
1000ng/ml
E
IgG2a
NIM-R5
Tumor volume, mm$^3$
300
250
200
150
100
50
0
*
*
*
0
5
10
15
20
↑
Days post-injection

**Figure 6**

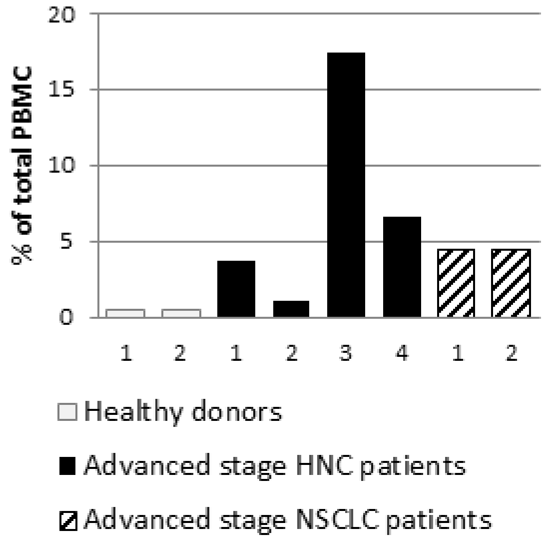
% of total PBMC
0
5
10
15
20
1
2
1
2
3
4
1
2
☐ Healthy donors
■ Advanced stage HNC patients
▨ Advanced stage NSCLC patients

Figure 7